Perturbative QCD factorization of $\pi\gamma^*\to\gamma(\pi)$ and $B\to\gamma(\pi)l\bar{\nu}$

Hsiang-nan Li
Department of Physics, National Cheng-Kung University, Tainan, Taiwan 701, Republic of China
and Physics Division, National Center for Theoretical Sciences, Hsinchu, Taiwan 300, Republic of China
(Received 27 December 2000; published 31 May 2001)

We prove the factorization theorem for the processes $\pi\gamma^*\to\gamma$ and $\pi\gamma^*\to\pi$ to leading twist in the covariant gauge by means of the Ward identity. Soft divergences cancel and collinear divergences are grouped into a pion wave function defined by a nonlocal matrix element. The gauge invariance and universality of the pion wave function are confirmed. The proof is then extended to the exclusive B meson decays $B\to\gamma l\bar{\nu}$ and $B\to\pi l\bar{\nu}$ in the heavy quark limit. It is shown that a light-cone B meson wave function, though absorbing soft dynamics, can be defined in an appropriate frame. Factorization of the $B\to\pi l\bar{\nu}$ decay in k_T space, k_T being parton transverse momenta, is briefly discussed. We comment on the extraction of the leading-twist pion wave function from experimental data.

DOI: 10.1103/PhysRevD.64.014019 PACS number(s): 12.38.Bx

I. INTRODUCTION

The fundamental concept of perturbative QCD (PQCD) is factorization theorem, which states that nonperturbative dynamics of a high-energy QCD process either cancel or can be absorbed into hadron wave functions. The remaining part, being infrared finite, is calculable in perturbation theory. A full amplitude is then expressed as the convolution of a hard amplitude with hadron wave functions. A wave function, because of its nonperturbative origin, is not calculable. However, PQCD still possesses a predictive power, since a wave function is universal, i.e., process independent. With this universality, a wave function determined by some means, such as QCD sum rules and lattice theory, or extracted from experimental data, can be employed to make predictions for other processes involving the same hadron.

Nonperturbative dynamics is reflected by infrared divergences in radiative corrections. There are two types of infrared divergences, soft and collinear. Soft divergences come from the region of a loop momentum l, where all its components vanish:

$$l^\mu=(l^+,l^-,l_T)\sim(\lambda,\lambda,\lambda). \tag{1}$$

The light-cone variables have been adopted, and λ is a small scale. Collinear divergences are associated with a massless quark of momentum $P=(Q,0,0_T)$, Q being a large scale. In the collienar region with l parallel to P, the components of l behave like

$$l^\mu\sim(Q,\lambda^2/Q,\lambda). \tag{2}$$

In both regions the invariant mass of the radiated gluon diminishes as λ^2, and the corresponding loop integrand may diverge as $1/\lambda^4$. As the phase space for loop integration vanishes like $d^4l\sim\lambda^4$, logarithmic divergences are generated.

Factorization of the above infrared divergences in a QCD process needs to be performed in momentum, spin, and color spaces. Factorization in momentum space means that a hard amplitude does not depend on the loop momentum of a soft or collinear gluon, which has been absorbed into a hadron wave function. Factorization in spin and color spaces means that there are separate fermion and color flows between a hard amplitude and a wave function, respectively. To achieve these, we rely on the eikonal approximation for loop integrals in leading infrared regions, the insertion of the Fierz identity to separate fermion flows, and the Ward identity to sum up diagrams with different color structures. Under the eikonal approximation, a soft or collinear gluon is detached from the lines in a hard amplitude and in other wave functions. The Fierz identity decomposes a full amplitude into contributions characterized by different twists. The Ward identity is essential for proving the factorization theorem in a non-Abelian gauge theory.

In this paper we shall derive the factorization of the scattering processes $\pi\gamma^*\to\gamma$ and $\pi\gamma^*\to\pi$, which involve the pion transition form factor and the pion form factor, respectively, at leading twist using the above techniques. Infrared divergences, occuring at higher powers of $1/Q^2$, Q being momentum transfer in the above processes, are neglected. It will be shown that soft divergences cancel and collinear divergences, factored out of the whole proesses order by order, are absorbed into a pion wave function, which is defined by a nonlocal matrix element. The universality of the pion wave function is equivalent to the universality of the collinear divergences in the two processes. The definition of the hard amplitude at each order will be given as a result of the proof. We emphasize that our derivation is simple, explicitly gauge-invariant, and appropriate for both the factorizations of the soft and collinear divergences.

The factorization of the process $\pi\gamma^*\to\gamma(\pi)$ has been proved in [1], but in the axial (light-cone) gauge $A^+=0$. In this gauge factorization automatically holds and the analysis is straightforward, because collinear divergences exist only in reducible diagrams. Our proof is performed in the covariant gauge, in which collinear divergences also exist in irreducible diagrams. The collection of these collinear gluons forms a path-ordered integral along the light cone, which renders a hadron wave function explicitly gauge invariant. The pion wave function has been constructed from $\gamma^*\gamma\to\pi$ in the framework of covariant operator product expan-

sion [2,3]. However, it was not clear how the path-ordered integral is generated [3]. We shall demonstrate that it appears as a consequence of the Ward identity. The factorization of $\pi\gamma^*\to\pi$ has also been proved in [4] based on a generalization of the Zimmermann's ''Δ-forest'' prescription [5], which involves complicated diagram subtractions. It will be found that our derivation is simpler.

We then prove factorization theorem for the exclusive B meson decays $B\to\gamma l\bar{\nu}$ and $B\to\pi l\bar{\nu}$, whose topologies are similar to the scattering processes $\pi\gamma^*\to\gamma$ and $\pi\gamma^*\to\pi$, respectively. The infrared divergences in $B\to\gamma l\bar{\nu}$ and $B\to\pi l\bar{\nu}$ have been investigated in [6] and [7], respectively. However, a rigorous proof of factorization theorem has not yet been available. In the heavy quark limit, terms of $O(\Lambda_{\rm QCD}/M_B)$, $\Lambda_{\rm QCD}$ being the QCD scale and M_B the B meson mass, are higher-twist and negligible. It will be shown that in this limit a gauge-invariant B meson wave function and hard amplitudes can be defined. The B meson wave function absorbs soft divergences of the above decays, which differ from the collinear divergences in the pion wave function. However, it is still possible to construct a light-cone B meosn wave function [8], if an appropriate frame with the photon (pion) moving in the minus or plus direction is chosen.

We investigate the $O(\alpha_s)$ collinear divergences contained in the process $\pi\gamma^*\to\gamma$ in Sec. II, and present the all-order proof of its factorization theorem by means of the Ward identity in Sec. III. The factorization of the process $\pi\gamma^*\to\pi$ is derived in Sec. IV. In Sec. V we prove factorization theorem for the $B\to\gamma l\bar{\nu}$ and $B\to\pi l\bar{\nu}$ decays. Section VI is the conclusion. The detailed evaluation of the $O(\alpha_s)$ collinear divergences in $\pi\gamma^*\to\pi$ are supplied in Appendix A. In Appendix B we comment on the extraction of the leading-twsit pion wave functions from experimental data of $\pi\gamma^*\to\gamma$ and $\pi\gamma^*\to\pi$.

II. $O(\alpha_s)$ FACTORIZATION OF $\pi\gamma^*\to\gamma$

We start with the factorization of the process $\pi\gamma^*\to\gamma$ at the one-loop level, which will serve as the basis of the all-order proof. The momentum P_1 of the pion and the momentum P_2 of the outgoing on-shell photon are parametrized as

$$P_1=(P_1^+,0,\mathbf{0}_T)=\frac{Q}{\sqrt{2}}(1,0,\mathbf{0}_T),$$

$$P_2=(0,P_2^-,\mathbf{0}_T)=\frac{Q}{\sqrt{2}}(0,1,\mathbf{0}_T). \tag{3}$$

Let ϵ denote the polarization vector of the outgoing photon, which contains only the transverse components. We consider the kinematic region with large $Q^2=-q^2$, $q=P_2-P_1$ being the virtual photon momentum, where PQCD is applicable.

The lowest-order diagrams are displayed in Fig. 1. The lower valence quark (an anti-quark) in the pion carries the fractional momentum xP_1. Contracting the amplitude in Fig. 1(a) with the leading-twist structure $\not{P}_1\gamma_5/\sqrt{2N_c}$ associated with the pion, $N_c=3$ being the number of colors, we derive

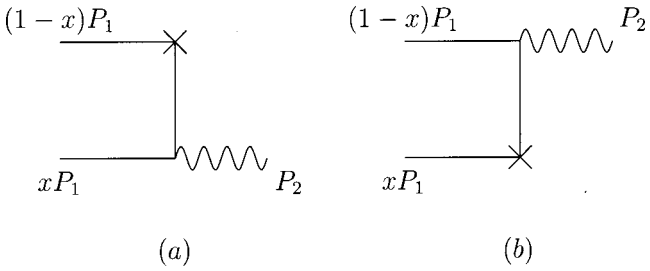

FIG. 1. Lowest-order diagrams for $\pi\gamma^*\to\gamma$ ($B\to\gamma l\bar{\nu}$), where the symbol $\times$ represents the virtual photon (weak decay) vertex.

$$H^{(0)}(x)=-ie^2\sqrt{\frac{N_c}{2}}\frac{\mathrm{tr}[\not{\epsilon}(\not{P}_2-x\not{P}_1)\gamma_\mu\not{P}_1\gamma_5]}{(P_2-xP_1)^2}$$

$$=ie^2\sqrt{\frac{N_c}{2}}\frac{\mathrm{tr}(\not{\epsilon}\not{P}_2\gamma_\mu\not{P}_1\gamma_5)}{xQ^2}. \tag{4}$$

Figure 1(b) leads to the same amplitude, because the pion wave function is symmetric under the interchange of x and $1-x$. The internal quarks are regarded as being hard, i.e., being off-shell by $O(Q^2)$, since contributions from the small x region will be suppressed by the pion wave function, which vanishes like x as $x\to 0$.

We identify the infrared divergences from $O(\alpha_s)$ radiative corrections [9–11] to Fig. 1(a), which are shown in Fig. 2. Self-energy correction to the internal quark, giving a next-to-leading-order hard amplitude, is not included. Figures 2(a)–2(c) are the reducible diagrams with the additional gluon attaching the two valence quarks of the pion. It has been known that soft divergences cancel among these diagrams. The reason for this cancellation is that soft gluons, being huge in space-time, do not resolve the color structure of the pion. Collinear divergences in Figs. 2(a)–2(c) do not cancel, since the loop momentum flows into the internal quark line in Fig. 2(b), but not in Figs. 2(a) and 2(c). To absorb the collinear divergences, we introduce a nonperturbative pion wave function.

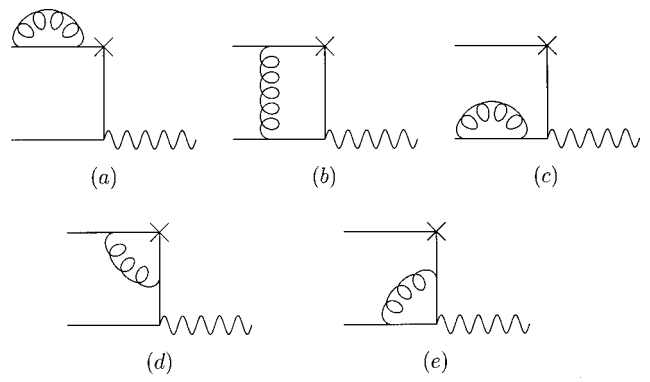

FIG. 2. $O(\alpha_s)$ radiative corrections to Fig. 1(a).

The factorization of Figs. 2(a)–2(c) is achieved by means of the insertion of the Fierz identity:

$$I_{ij}I_{lk}=\frac{1}{4}I_{ik}I_{lj}+\frac{1}{4}(\gamma_5)_{ik}(\gamma_5)_{lj}+\frac{1}{4}(\gamma_\alpha)_{ik}(\gamma^\alpha)_{lj}+\frac{1}{4}(\gamma_5\gamma_\alpha)_{ik}(\gamma^\alpha\gamma_5)_{lj}+\frac{1}{8}(\sigma_{\alpha\beta})_{ik}(\sigma^{\alpha\beta})_{lj}, \quad (5)$$

where I represents the identity matrix, and $\sigma_{\alpha\beta}$ is defined by $\sigma_{\alpha\beta}\equiv i[\gamma_\alpha,\gamma_\beta]/2$. Different terms in the above identity lead to contributions of different twists. Take Fig. 2(b) as an example, whose loop integrand is given by

$$I_{2b}=e^2g^2C_F\sqrt{\frac{N_c}{2}}\mathrm{tr}\left\{\gamma_\nu\frac{x\not P_1-\not l}{(xP_1-l)^2}\not\epsilon\frac{\not P_2-x\not P_1+\not l}{(P_2-xP_1+l)^2}\gamma_\mu\times\frac{(1-x)\not P_1+\not l}{[(1-x)P_1+l]^2}\gamma^\nu\not P_1\gamma_5\right\}\frac{1}{l^2}, \quad (6)$$

with C_F being a color factor. Inserting the Fierz identity, we obtain

$$I_{2b}\approx ig^2C_F\,\mathrm{tr}\left\{\gamma_\nu\frac{x\not P_1-\not l}{(xP_1-l)^2}\frac{\gamma_5\gamma_\alpha}{2}\times\frac{(1-x)\not P_1+\not l}{[(1-x)P_1+l]^2}\gamma^\nu\frac{\gamma^-\gamma_5}{2}\right\}\frac{1}{l^2}(-ie^2)\sqrt{\frac{N_c}{2}}\times\frac{\mathrm{tr}[\not\epsilon(\not P_2-x\not P_1+\not l)\gamma_\mu\gamma^\alpha\gamma_5)P_1^+}{(P_2-xP_1+l)^2}. \quad (7)$$

Obviously, in the collinear region with the loop momentum l parallel to P_1, only the pseudo-vector structure $\gamma_5\gamma_\alpha$ contributes to the first trace as shown above. Moreover, the matrices γ_α and γ^α must be $\gamma_-=\gamma^+$ and γ^-, respectively.

Equation (7), as integrated over l, is rewritten as the convolution of the lowest-order hard amplitude $H^{(0)}(\xi)$ with the $O(\alpha_s)$ pion wave function $\phi_{2b}^{(1)}$ in the momentum fraction $\xi=x-l^+/P_1^+$:

$$I_{2b}\approx\phi_{2b}^{(1)}H^{(0)}(\xi), \quad (8)$$

$$\phi_{2b}^{(1)}=ig^2C_F\,\mathrm{tr}\left\{\gamma_\nu\frac{x\not P_1-\not l}{(xP_1-l)^2}\frac{\gamma_5\gamma^+}{2}\times\frac{(1-x)\not P_1+\not l}{[(1-x)P_1+l]^2}\gamma^\nu\frac{\gamma^-\gamma_5}{2}\right\}\frac{1}{l^2}. \quad (9)$$

$\phi_{2b}^{(1)}$ contains the collinear divergence in Fig. 2(b), because the integrand in Eq. (9) diverges as $1/\lambda^4$. The dependences on l^- and on l_T in $H^{(0)}$, being subleading according to Eq. (2), have been neglected.

Diagrams with the additional gluon attaching the internal quark, Figs. 2(d) and 2(e), do not contain soft divergences, because the internal quark is off-shell. For example, the loop integrand corresponding to Fig. 2(d) is approximated, in the $l\to0$ region, by

$$\frac{1}{(P_2-xP_1+l)^2[(1-x)P_1+l]^2l^2}\approx\frac{1}{2(1-x)(P_2-xP_1)^2P_1\cdot ll^2}\sim O(\lambda^{-3}), \quad (10)$$

which is suppressed by the phase space for loop integration $d^4l\sim\lambda^4$. Therefore, we consider only the collinear divergences. The integrand associated with Fig. 2(d) is written as

$$I_{2d}=-e^2g^2C_F\sqrt{\frac{N_c}{2}}\mathrm{tr}\left\{\not\epsilon\frac{\not P_2-x\not P_1}{(P_2-xP_1)^2}\gamma_\nu\frac{\not P_2-x\not P_1+\not l}{(P_2-xP_1+l)^2}\gamma_\mu\times\frac{(1-x)\not P_1+\not l}{[(1-x)P_1+l]^2}\gamma^\nu\not P_1\gamma_5\right\}\frac{1}{l^2}. \quad (11)$$

Since $\not\epsilon$ and γ_μ involve only γ_T, we drop $-x\not P_1$ and $-x\not P_1+\not l$ in the internal quark propagators in the collinear region. Equation (11) is then simplified into

$$I_{2d}=-e^2g^2C_F\sqrt{\frac{N_c}{2}}\frac{2P_{2\nu}}{(P_2-xP_1+l)^2}\times\mathrm{tr}\left\{\not\epsilon\frac{\not P_2-x\not P_1}{(P_2-xP_1)^2}\gamma_\mu\frac{(1-x)\not P_1+\not l}{[(1-x)P_1+l]^2}\gamma^\nu\not P_1\gamma_5\right\}\frac{1}{l^2}. \quad (12)$$

For the l-dependent hard propagator, we employ the relation

$$\frac{2P_{2\nu}}{(P_2-xP_1+l)^2}\approx\frac{n_\nu}{n\cdot l}\left[1-\frac{(P_2-xP_1)^2}{(P_2-xP_1+l)^2}\right], \quad (13)$$

which is an example of the Ward identity. The dimensionless vector $n=P_2/P_2^-$, representing the direction of an eikonal line, lies along the outgoing photon momentum. n_ν is called the eikonal vertex and $1/n\cdot l$ is called the eikonal propagator. The appearence of the eikonal line is a consequence of the Ward identity. Inserting the Fierz identity, we derive the factorization,

$$I_{2d}\approx\phi_{2d}^{(1)}[H^{(0)}(x)-H^{(0)}(\xi)], \quad (14)$$

with the $O(\alpha_s)$ pion wave function

$$\phi_{2d}^{(1)}=-ig^2C_F\,\mathrm{tr}\left\{\frac{\gamma_5\gamma^+}{2}\frac{(1-x)\not P_1+\not l}{[(1-x)P_1+l]^2}\gamma^\nu\frac{\gamma^-\gamma_5}{2}\right\}\frac{1}{l^2}\frac{n_\nu}{n\cdot l}. \quad (15)$$

The collinear contribution from Fig. 2(d) has been split into two terms, with the first and second terms described by Figs. 3(a) and 3(b), respectively, where the eikonal propagator is represented by a double line. In Fig. 3(b) the loop momen-

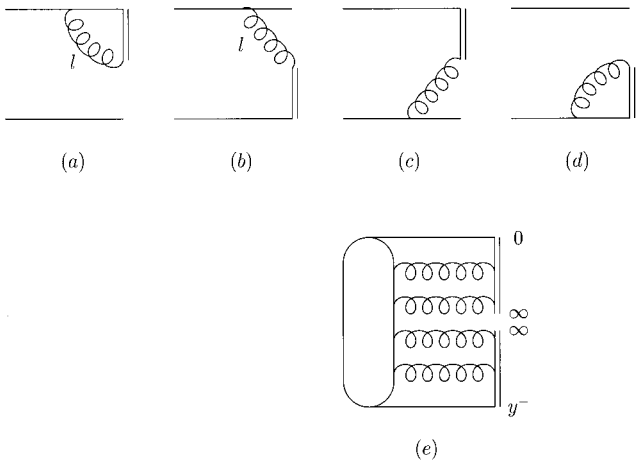

FIG. 3. (a)–(d) Infrared divergent diagrams factored out of Figs. 2(d) and 2(e). (e) The graphic definition of the leading-twist pion wave function.

tum l flows into the internal quark line, such that the second term is a convolution of $H^{(0)}$ with $\phi_{2d}^{(1)}$ in the momentum fraction ξ.

Figure 2(e) gives the loop integrand

$$I_{2e}=e^2g^2C_F\sqrt{\frac{N_c}{2}}\mathrm{tr}\left\{\gamma^\nu\frac{x\not P_1-\not l}{(xP_1-l)^2}\not\epsilon\frac{\not P_2-x\not P_1+\not l}{(P_2-xP_1+l)^2}\gamma_\nu \times\frac{\not P_2-x\not P_1}{(P_2-xP_1)^2}\gamma_\mu\not P_1\gamma_5\right\}\frac{1}{l^2}. \tag{16}$$

Following the similar procedures, we obtain, in the collinear region,

$$I_{2e}\approx-\phi_{2e}^{(1)}[H^{(0)}(\xi)-H^{(0)}(x)], \tag{17}$$

with the $O(\alpha_s)$ pion wave function

$$\phi_{2e}^{(1)}=ig^2C_F\,\mathrm{tr}\left\{\gamma^\nu\frac{\not P_1-\not l}{(xP_1-l)^2}\frac{\gamma_5\gamma^+}{2}\frac{\gamma^-\gamma_5}{2}\right\}\frac{1}{l^2}\frac{n_\nu}{n\cdot l}. \tag{18}$$

The first and second terms in Eq. (17) are described by Figs. 3(c) and 3(d), respectively.

Comparing Eqs. (9), (15), and (18), the Feynman rules for the perturbative evaluation of the pion wave function are clear: $\phi^{(1)}$ can be written as a nonlocal hadronic matrix element with the structure $\gamma_5\gamma^+/2$ sandwiched, which comes from the insertion of the Fierz identity:

$$\phi^{(1)}(x)=\frac{1}{\sqrt{2N_c}P_1^+}\int\frac{dy^-}{2\pi}e^{ixP_1^+y^-}\langle0|\overline{q}(y^-)\frac{\gamma_5\gamma^+}{2}(-ig) \times\int_0^{y^-}dzn\cdot A(zn)q(0)|\pi(P_1)\rangle. \tag{19}$$

The sum over colors is understood. The integral over z in fact contains two pieces: For the upper eikonal line in Fig. 3(a), z runs from 0 to ∞. For the lower eikonal line in Fig. 3(b), z runs from ∞ back to y^-. It is easy to confirm that the above definition reproduces all the leading-twist collinear divergences in Figs. 2(a)–2(c) and in Figs. 3(a)–3(d). The light-cone coordinate $y^-\neq0$ corresponds to the fact that the collinear divergences in Fig. 2 do not cancel exactly.

At last, the factorization formula for the process $\pi\gamma^*\to\gamma$ is written, up to $O(\alpha_s)$, as

$$(\phi^{(0)}+\phi^{(1)})\otimes(H^{(0)}+H^{(1)})+O(\alpha_s^2), \tag{20}$$

with $\phi^{(0)}=1$ and $\otimes$ representing the convolution in the momentum fraction. The $O(\alpha_s)$ hard amplitude $H^{(1)}$ is defined by

$$H^{(1)}\equiv\sum_i\int\frac{d^4l}{(2\pi)^4}I_i-\phi^{(1)}\otimes H^{(0)}, \tag{21}$$

where the subscript i runs from $2a$ to $2e$. Obviously, $H^{(1)}$ is infrared finite, since all the (α_s) collinear divergences have been absorbed into the pion wave function $\phi^{(1)}$.

III. ALL-ORDER PROOF OF FACTORIZATION THEOREM

In this section we present the all-order proof of leading-twist factorization theorem for the process $\pi\gamma^*\to\gamma$, and construct a gauge-invariant pion wave function defined by

$$\phi(x)=\frac{1}{\sqrt{2N_c}P_1^+}\int\frac{dy^-}{2\pi}e^{ixP_1^+y^-}\langle0|\overline{q}(y^-)\frac{\gamma_5\gamma^+}{2}P \times\exp\left[-ig\int_0^{y^-}dzn\cdot A(zn)\right]q(0)|\pi(P_1)\rangle, \tag{22}$$

as shown in Fig. 3(e). The notation P means the path ordering. By expanding the quark field $\overline{q}(y^-)$ and the path-ordered exponential into powers of y^-, the above matrix element can be expressed as a series of covariant derivatives $(D^+)^n\overline{q}(0)$, implying that Eq. (22) is gauge invariant.

It has been mentioned in the Introduction that factorization of a QCD process in momentum, spin, and color spaces requires summations of many diagrams, especially at higher orders. Hence, the diagram summation must be handled in an elegant way. For this purpose, we employ the Ward identity,

$$l_\mu G^\mu(l,k_1,k_2,\ldots,k_n)=0, \tag{23}$$

where G^μ represents a physical amplitude with an external gluon carrying the momentum l and with n external quarks carrying the momenta k_1, $k_2,\ldots,k_n$. All these external particles are on mass shell. The Ward identity can be easily derived by means of the Becchi-Rouet-Stora (BRS) transformation [12].

We prove factorization theorem by induction. The factorization of the $O(\alpha_s)$ collinear divergences associated with the pion has been worked out in Sec. II. Assume that the factorization holds up to $O(\alpha_s^N)$:

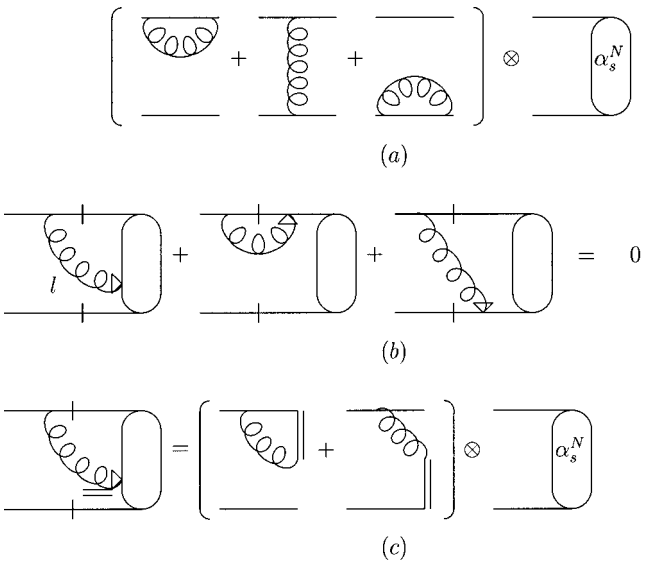

FIG. 4. (a) Factorization of $O(\alpha_s^{N+1})$ reducible diagrams. (b) The Ward identity. (c) Factorization of $O(\alpha_s^{N+1})$ irreducible diagrams.

$$G=\phi\otimes H, \tag{24}$$

with

$$G=\sum_{i=0}^{N} G^{(i)}, \quad \phi=\sum_{i=0}^{N} \phi^{(i)}, \quad H=\sum_{i=0}^{N} H^{(i)}. \tag{25}$$

$G^{(i)}$ denotes the full diagrams of $O(\alpha_s^i)$ with $G^{(0)}=H^{(0)}$ in Eq. (4), the pion wave function $\phi^{(i)}$ is defined by the $O(\alpha_s^i)$ terms in the perturbative expansion of Eq. (22), and $H^{(i)}$ is the infrared-finite hard amplitude of $O(\alpha_s^i)$. We then have the relations

$$G^{(i)}=\sum_{j=0}^{i} \phi^{(j)}\otimes H^{(i-j)}, \tag{26}$$

for $i=0,\ldots,N$, which imply that all collinear divergences in $G^{(i)}$ have been collected into $\phi^{(j)}$, $j\leqslant i$, systematically.

Consider a complete set of full diagrams $G^{(N+1)}$ of $O(\alpha_s^{N+1})$. We look for the gluon, one of whose ends attaches the outer most vertex on the upper quark line in the pion. Such a gluon exists, since $G^{(N+1)}$ are finite-order diagrams. We then classify $G^{(N+1)}$ into two categories, reducible and irreducible, according to the attachment of the other end of this gluon. If the other end attaches the upper or lower quark lines directly, the diagrams are reducible. The $O(\alpha_s)$ examples are Figs. 2(a)–2(c). All other diagrams, with the other end attaching inside of the $O(\alpha_s^N)$ full diagrams $G^{(N)}$, are irreducible. The $O(\alpha_s)$ examples are Figs. 2(d) and 2(e). The factorization of reducible diagrams is the same as that of Figs. 2(a)–2(c): we simply insert the Fierz identity to separate $G^{(N+1)}$ into the convolution of $G^{(N)}$ with the $O(\alpha_s)$ collinear divergent diagrams, which contribute to the pion wave function $\phi^{(1)}$. The result is shown in Fig. 4(a). The explicit expression of $\phi_{2b}^{(1)}$ has been derived in Eq. (9).

We then discuss factorization of irreducible $G^{(N+1)}$. Let α be the outer most vertex on the upper quark line, and β denote the attachments of the other end of the radiated gluon inside $G^{(N)}$. The pion possesses the leading-twist spin structure $\not{P}_1\gamma_5$ from the Fierz identity. The fermion propagator adjacent to the vertex α is proportional to $\not{P}_1$ in the collinear region with the loop momentum l parallel to P_1. Hence, the component γ^+ in γ^α, which is located between the spin structure and the fermion propagator, gives the leading contribution. The vertex β must be dominated by the minus component. With the above reasoning, we propose the following replacement for the tensor $g^{\alpha\beta}$ appearing in the propagator of the radiated gluon:

$$g_{\alpha\beta}\to\frac{n_\alpha l_\beta}{n\cdot l}. \tag{27}$$

The lightlike vector n_α in the minus direction, which was introduced in Eq. (13), selects the plus component of γ^α. In the collinear region l lies mainly in the plus direction, and l_β selects the minus component of the vertex β. Therefore, Eq. (27) extracts the leading-twist collinear divergences from the irreducible $G^{(N+1)}$.

The contraction of l^β hints the application of the Ward identity in Eq. (23) to the case with two external on-shell quarks. Figure 4(b) contains a complete set of contractions of l^β, which are represented by arrows, since the second and third diagrams have been added. The cuts on the quark lines denote the insertion of the Fierz identity. The Ward identity, namely, the equation described by Fig. 4(b), holds. The second diagram gives

$$\begin{aligned} l_\beta\frac{1}{(1-x)\not{P}_1-\not{l}}\gamma^\beta\not{P}_1\gamma_5 &= \frac{1}{(1-x)\not{P}_1-\not{l}}[\not{l}-(1-x)\not{P}_1+(1-x)\not{P}_1]\not{P}_1\gamma_5 \\ &= \frac{(1-x)P_1^2\gamma_5}{(1-x)\not{P}_1-\not{l}}-\not{P}_1\gamma_5. \end{aligned} \tag{28}$$

The first term in the second expression vanishes because of the on-shell condition $P_1^2=0$. The second term corresponds to the $O(\alpha_s^N)$ full diagrams $G^{(N)}$. Similarly, the third diagram leads to

$$l_\beta\not{P}_1\gamma_5\gamma^\beta\frac{1}{x\not{P}_1-\not{l}}=-\frac{xP_1^2\gamma_5}{x\not{P}_1-\not{l}}-\not{P}_1\gamma_5, \tag{29}$$

where the first term vanishes and the second term corresponds to $G^{(N)}$. The factor $n_\alpha/n\cdot l$ from the collinear replacement in Eq. (27) is exactly the Feynman rule associated with the eikonal line in the direction of n. Equations (28) and (29) imply that in the collinear region the irreducible $G^{(N+1)}$ are factorized as shown in Fig. 4(c). Obviously, the factorization of the irreducible diagrams with the gluon emitted from the outer most vertex on the lower quark line exists. We conclude that the irreducible $G^{(N+1)}$ can be factorized

into the convolution of $G^{(N)}$ with $\phi^{(1)}$ described by Figs. 3(a)–3(d), in which the radiated gluon attaches the eikonal lines.

We derive the collinear factorization of $G^{(N+1)}$:

$$G^{(N+1)} \approx \phi^{(1)} \otimes G^{(N)}, \tag{30}$$

where $\phi^{(1)}$ contains both the reducible gluons in Fig. 4(a) and the irreducible gluons in Figs. 3(a)–3(d). The remaining part $F^{(N+1)}$, defined via

$$G^{(N+1)} = \phi^{(1)} \otimes G^{(N)} + F^{(N+1)}, \tag{31}$$

is infrared finite, i.e., free from the collinear divergence associated with the pion. The above procedures are also applicable to the $O(\alpha_s^{N+1})$ pion wave function $\phi^{(N+1)}$, which is defined by the perturbative expansion of Eq. (22). We have

$$\phi^{(N+1)} = \phi^{(1)} \otimes \phi^{(N)} + \overline{F}^{(N+1)}, \tag{32}$$

with the infrared-finite function $\overline{F}^{(N+1)}$.

Employing Eqs. (26), (31), and (32), we write

$$\begin{aligned} G^{(N+1)} &= \phi^{(1)} \otimes \sum_{j=0}^{N} \phi^{(j)} \otimes H^{(N-j)} + F^{(N+1)} \\ &= \sum_{j=0}^{N} [\phi^{(j+1)} - \overline{F}^{(j+1)}] \otimes H^{(N-j)} + F^{(N+1)} \\ &= \sum_{j=1}^{N+1} \phi^{(j)} \otimes H^{(N+1-j)} + H^{(N+1)}, \end{aligned} \tag{33}$$

with the $O(\alpha_s^{N+1})$ hard amplitude,

$$H^{(N+1)} \equiv F^{(N+1)} - \sum_{j=1}^{N} \overline{F}^{(j+1)} \otimes H^{(N-j)}. \tag{34}$$

Obviously, the function $H^{(N+1)}$ does not contain any collinear divergence, since both F and $\overline{F}$ are infrared finite. Because of $\phi^{(0)}=1$, Eq. (33) becomes

$$G^{(N+1)} = \sum_{j=0}^{N+1} \phi^{(j)} \otimes H^{(N+1-j)}. \tag{35}$$

The above expression indicates that all collinear divergences in the full diagrams of $\pi\gamma^* \to \gamma$ can be factored into the definition of the pion wave function in Eq. (22) order by order, and that the remaining hard amplitude is infrared finite. Allowing N to approach infinity, we prove factorization theorem for the process $\pi\gamma^* \to \gamma$ to all orders.

At last, we prove by induction that soft divergences do not exist in the process $\pi\gamma^* \to \gamma$ to leading twist. The $O(\alpha_s)$ soft cancellation has been explained in Sec. II. Assume that the $O(\alpha_s^N)$ full diagrams $G^{(N)}$ do not contain any soft divergence (though they contain collinear divergences). Consider the $O(\alpha_s^{N+1})$ full diagrams $G^{(N+1)}$. Similarly, we look for the gluon radiated from the outer most vertex on the upper quark line, and classify the diagrams into the reducible and irreducible types. For reducible diagrams, we express $G^{(N+1)}$ as the convolution of $G^{(N)}$ with the $O(\alpha_s)$ infrared divergent diagrams as shown in Fig. 4(a). It is easy to confirm that the derivation in Eqs. (6)–(8) still applies to the soft region with the loop momentum $l \to 0$. The soft divergences in the $O(\alpha_s)$ diagrams cancel in the same way as in Figs. 2(a)–2(c). The remaining $G^{(N)}$ are free from soft divergences as assumed above. Hence, the reducible $G^{(N+1)}$ have no soft divergences.

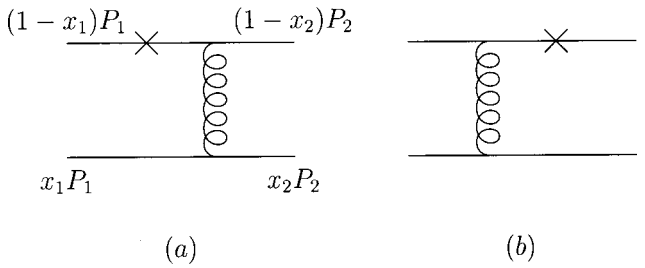

FIG. 5. Lowest-order diagrams for $\pi\gamma^* \to \pi$ ($B \to \pi l \overline{\nu}$), where the symbol $\times$ represents the virtual photon (weak decay) vertex.

We then consider irreducible $G^{(N+1)}$. The diagrams $G^{(N)}$, without soft divergences, are dominated either by hard or by collinear dynamics. In the hard region of $G^{(N)}$, internal particle propagators behave like $1/Q^2$. The attachment of a soft gluon, producing one more hard propagator, does not introduce soft divergences. The reason for this absence of soft divergences is the same as in Eq. (10). In the collinear region of $G^{(N)}$, where momenta parallel to P_1 dominate, we employ the eikonal approximation for the small loop momentum l,

$$\frac{\not{P}_1 + \not{l}}{(P_1+l)^2} \gamma_\alpha \not{P}_1 \approx \frac{P_{1\alpha}}{P_1 \cdot l} \not{P}_1. \tag{36}$$

The contraction of the numerator $P_{1\alpha}$ to the outer most vertex γ^α, which is mainly γ^+, leads to a vanishing contribution. Therefore, the irreducible $G^{(N+1)}$ do not contain soft divergences either. Extending N to infinity, we prove that the process $\pi\gamma^* \to \gamma$ is free from soft divergences.

IV. FACTORIZATION OF $\pi\gamma^* \to \pi$

We investigate infrared divergences in the process $\pi\gamma^* \to \pi$, and discuss only the factorization of the initial-state pion wave function. The discussion of the final-state wave function is the same. Assume that the incoming and outgoing pions carry the momenta P_1 and P_2, respectively, which are defined by Eq. (3), and that the momentum fraction x_1 (x_2) is associated with the lower quark line in the incoming (outgoing) pion. The above kinematic variables have been indicated in the lowest-order diagrams in Fig. 5. Similarly, we consider the region with large momentum transfer $Q^2 = -q^2$, $q = P_2 - P_1$ being the virtual photon momentum.

Contracting the four-quark amplitudes in Fig. 5 with the leading-twist spin structures $\not{P}_1\gamma_5/\sqrt{2N_c}$ and $\gamma_5\not{P}_2/\sqrt{2N_c}$ from the initial and final states, respectively, we derive

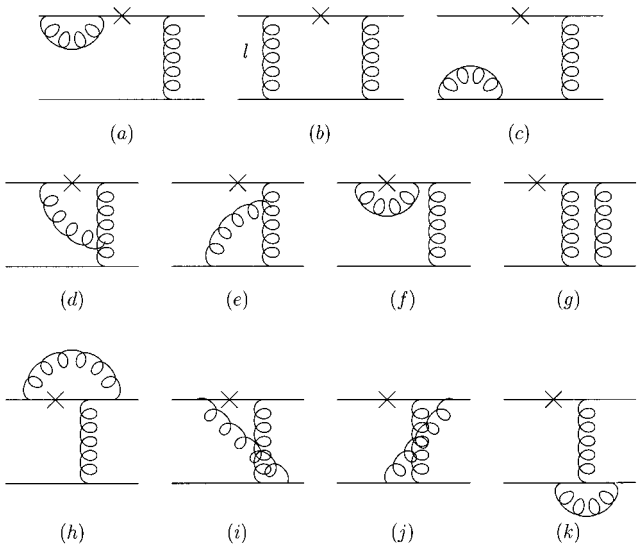

FIG. 6. $O(\alpha_s)$ radiative corrections to Fig. 5(a).

$$H_{5a}^{(0)}(x_1,x_2)=\frac{i}{2}eg^2C_F\frac{\mathrm{tr}[\gamma^\nu\gamma_5\not{P}_2\gamma_\nu(\not{P}_2-x_1\not{P}_1)\gamma_\mu\not{P}_1\gamma_5]}{(P_2-x_1P_1)^2(x_1P_1-x_2P_2)^2}$$

$$=-\frac{4eg^2C_F}{x_1x_2Q^2}iP_{1\mu}, \tag{37}$$

$$H_{5b}^{(0)}(x_1,x_2)=\frac{i}{2}eg^2C_F\frac{\mathrm{tr}[\gamma^\nu\gamma_5\not{P}_2\gamma_\mu(\not{P}_1-x_2\not{P}_2)\gamma_\nu\not{P}_1\gamma_5]}{(P_1-x_2P_2)^2(x_1P_1-x_2P_2)^2}$$

$$=-\frac{4eg^2C_F}{x_1x_2Q^2}iP_{2\mu}. \tag{38}$$

The other two lowest-order diagrams, where the virtual photon attaches the lower quark lines, lead to the same expressions but with different electric charge e. Since contributions from soft partons ($x_1,x_2\to0$) are suppressed by the pion wave functions, the exchanged gluons in Fig. 5, off-shell by $O(Q^2)$, are regarded as being hard.

A. $O(\alpha_s)$ factorization

We first identify infrared divergences from $O(\alpha_s)$ radiative corrections [13] to Fig. 5(a). The diagrams in Fig. 6 contain potential infrared divergences associated with the incoming pion. We do not consider self-energy corrections to the inernal lines, since they, without infrared divergences, give only a next-to-leading-order hard amplitude. The treatment of Figs. 6(a)–6(c) is the same as that of Figs. 2(a)–2(c): soft divergences cancel and collinear divergences are factored into the pion wave function $\phi^{(1)}$ by inserting the Fierz identity.

Diagrams with the additional gluon attaching the internal lines, such as Figs. 6(d)–6(g), do not generate soft divergences, because the internal lines are off-shell. We concentrate only on collinear divergences. Following the detailed calculation in Appendix A, the collinear divergences in Figs. 6(d) and 6(e) are given by

$$I_{6d}\approx\frac{N_c}{2C_F}\phi_{2d}^{(1)}[H_{5a}^{(0)}(x_1,x_2)-H_{5a}^{(0)}(\xi_1,x_2)], \tag{39}$$

$$I_{6e}\approx\frac{N_c}{2C_F}\phi_{2e}^{(1)}[H_{5a}^{(0)}(x_1,x_2)-H_{5a}^{(0)}(\xi_1,x_2)], \tag{40}$$

with $\xi_1=x_1-l^+/P_1^+$. The dependences on l^- and l_T in $H_{5a}^{(0)}$ have been neglected, since they are subleading in the collinear region. Collinear divergences from l parallel to P_1 vanish in Figs. 6(f) and 6(g). We have separated the integrands I_{6d} and I_{6e} into two terms, similar to those in Eqs. (14) and (17). However, the color factors are different because of the different color flows in Figs. 2(d) and 6(d). We shall explain how to fix the color factors after calculating Figs. 6(h)–6(k).

The collinear factorization of the irreducible corrections in Figs. 6(h)–6(k) relies on the eikonal approximation. The results are written as

$$I_{6h}\approx-\frac{1}{2C_FN_c}\phi_{2d}^{(1)}H_{5a}^{(0)}(x_1,x_2), \tag{41}$$

$$I_{6i}\approx\frac{1}{2C_FN_c}\phi_{2d}^{(1)}H_{5a}^{(0)}(\xi_1,x_2), \tag{42}$$

$$I_{6j}\approx\frac{1}{2C_FN_c}\phi_{2e}^{(1)}H_{5a}^{(0)}(\xi_1,x_2), \tag{43}$$

$$I_{6k}\approx-\frac{1}{2C_FN_c}\phi_{2e}^{(1)}H_{5a}^{(0)}(x_1,x_2). \tag{44}$$

To discuss soft divergences, we simply allow l^+ to appraoch zero, i.e., $\xi_1\to x_1$. It is easy to find that soft divergences cancel between Figs. 6(h) and 6(i) and between Figs. 6(j) and 6(k). Hence, irreducible corrections are free from soft divergences.

Combining Eq. (41) and Eq. (42) with the first and second terms in Eq. (39), respectively, and combining Eq. (43) and Eq. (44) with the second and first terms in Eq. (40), respectively, we obtain the correct color factors:

$$I_{6(d)-6(k)}\approx\phi_{2d}^{(1)}[H_{5a}^{(0)}(x_1,x_2)-H_{5a}^{(0)}(\xi_1,x_2)]+\phi_{2e}^{(1)}[H_{5a}^{(0)}(x_1,x_2)-H_{5a}^{(0)}(\xi_1,x_2)], \tag{45}$$

which are also described by Figs. 3(a)–3(d). It is observed from the above expression that the collinear divergences in the summation of Figs. 6(d)–6(k) are identical to those in the summation of Figs. 2(d) and 2(e), consistent with the universality of hadron wave functions.

We then investigate infrared divergences from radiative corrections to Fig. 5(b). The diagrams in Fig. 7 contain potential infrared divergences associated with the incoming pion. The factorization of Figs. 7(a)–7(c) is the same as that of Figs. 6(a)–6(c): They are absorbed into the leading-twist pion wave function $\phi^{(1)}$ straightforwardly. The contributions from Figs. 7(d) and 7(e) are the same as those from Figs. 6(d) and 6(e).

For Figs. 7(f), we consider only the collinear divergences from l parallel to P_1,

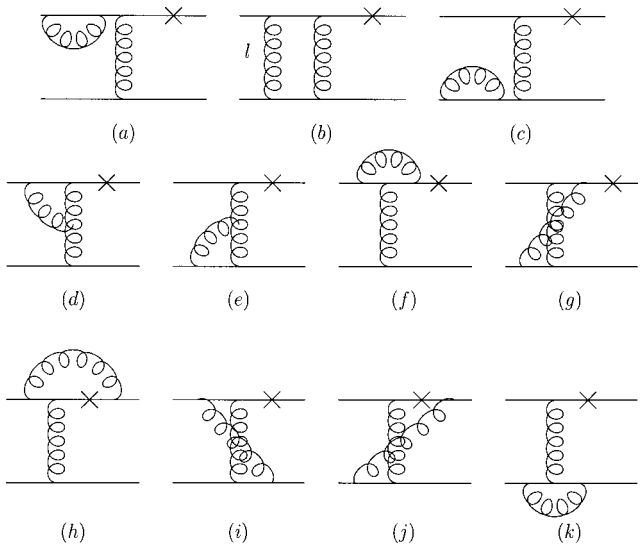

FIG. 7. $O(\alpha_s)$ radiative corrections to Fig. 5(b).

$$I_{7f} \approx \frac{ig^2}{N_c} \frac{n\cdot[(1-x_1)P_1+l]}{[(1-x_1)P_1+l]^2 l^2 n\cdot(P_1+l)} H_{5b}^{(0)}(x_1,x_2). \tag{46}$$

The result differs form that of Fig. 6(f), which vanishes. Note that the collinear divergence in Eq. (46) is not in the correct eikonal form. To show that it does not cause any trouble, we consider the collinear factorization of Fig. 7(h),

$$I_{7h} \approx \frac{ig^2}{N_c} \frac{n\cdot[(1-x_1)P_1+l]}{[(1-x_1)P_1+l]^2 l^2 n\cdot(P_1+l)} \frac{n\cdot P_1}{n\cdot l} H_{5b}^{(0)}(x_1,x_2). \tag{47}$$

Combining Eqs. (46) and (47), we have the simpler expression

$$I_{7f+7h} \approx -\frac{1}{2C_F N_c} \phi_{2d}^{(1)} H_{5b}^{(0)}(x_1,x_2), \tag{48}$$

whose collinear divergence is exactly the same as that of Fig. 6(h) in Eq. (41). At last, combining the collinear divergences in Eq. (48) and those from Fig. 7(d), we obtain the result described by Fig. 3(a).

A similar analysis shows that the collinear divergences in the sum of Figs. 7(g) and 7(j) are the same as in Fig. 6(j). Combined with the divergences from Fig. 7(e), we obtain the result described by Fig. 3(c). The results for Figs. 7(i) and 7(k) are the same as for Figs. 6(i) and 6(k), respectively, and their collinear factorizations, combined with Figs. 7(d) and 7(e), are described by Figs. 3(b) and 3(d), respectively. We conclude that the $O(\alpha_s)$ collinear divergences in Figs. 6 and 7 are identical to those in Fig. 2, and can be formulated into the leading-twist pion wave function $\phi^{(1)}$ defined in Eq. (19).

B. All-order factorization

The analysis of the $O(\alpha_s)$ collinear divergences in $\pi\gamma^* \to \pi$ indicates that factorization of a QCD process requires summations of many diagrams. For example, the summation of Figs. 7(f) and 7(h) removes the dependence of the hard amplitude on the loop momentum l. The summations of Figs. 6(d) and 6(h) and of Figs. 7(d), 7(f), and 7(h) give the correct color factors. To prove factorization theorem to all orders, we deal with these summations by means of the Ward identity. It is trivial to generalize the proof for the process $\pi\gamma^* \to \gamma$ to $\pi\gamma^* \to \pi$. In the present case the amplitude G^μ in Eq. (23) contains four external on-shell quarks. We simply interpret the function H as the part that does not involve the collinear divergences associated with the incoming pion. Then repeat the procedures and further factorize H into the the convolution of a hard amplitude with the wave function associated with the outgoing pion.

The proof of the absence of soft divergences in the process $\pi\gamma^* \to \pi$ is subtler. It has been shown that the $O(\alpha_s)$ corrections do not produce soft divergences. Assume that the soft cancellation exists up to $O(\alpha_s^N)$. For reducible $O(\alpha_s^{N+1})$ full diagrams $G^{(N+1)}$, we insert the Fierz identity to factor out the $O(\alpha_s)$ infrared divergent diagrams, which involve the gluons emitted from the outer most vertices on the upper and lower quark lines. This insertion works for both the initial- and final-state pions. The soft divergences in the $O(\alpha_s)$ diagrams cancel in the same way as in Figs. 2(a)–2(c). The remaining $O(\alpha_s^N)$ full diagrams $G^{(N)}$ have no soft divergences as assumed above. Hence, the reducible $G^{(N+1)}$ do not contain soft divergences.

For irreducible $G^{(N+1)}$, we consider the gluon emitted from the outer most vertices on the upper and lower quark lines in the incoming pion. Since $G^{(N)}$ are free from soft divergences, they are dominated either by hard or by collinear dynamics. In the hard region and in the collinear region with momenta parallel to P_1, the soft divergences vanish for the same reason as for the process $\pi\gamma^* \to \gamma$. In the collinear region with momenta parallel to P_2, we adopt the eikonal approximation,

$$\frac{\not P_2 + \not l}{(P_2+l)^2} \gamma_\alpha \not P_2 \approx \frac{n_\alpha}{n\cdot l} \not P_2. \tag{49}$$

It is easy to observe that the above approximation can be achieved by the replacement in Eq. (27).

We propose to employ Eq. (27) to extract the soft divergences in the irreducible $G^{(N+1)}$. In the hard region and in the collinear region with momenta parallel to P_1, the replacement in Eq. (27) simply modifies subleading contributions, that are free from soft divergences. In the collinear region with momenta parallel to P_2, the replacement extracts the correct soft divergences in the irreducible $G^{(N+1)}$. Hence, Eq. (27) always works for a leading-twist analysis of soft divergences. The derivation from Eq. (28) to Eq. (30) holds, and the irreducible $G^{(N+1)}$ are factorized into the convolution of $G^{(N)}$ with Figs. 3(a)–3(d). Since $G^{(N)}$ have no soft divergences, we allow the loop momentum l flowing inside $G^{(N)}$ to approach zero. It is then obvious that the soft

divergences cancel between Figs. 3(a) and 3(b) and between Figs. 3(c) and 3(d). That is, the irreducible $G^{(N+1)}$, like the reducible $G^{(N+1)}$, are also free from soft divergences. The same argument applies to the gluons emitted from the outgoing pion side. At last, extending N to infinity, we prove the absence of soft divergences in the process $\pi\gamma^*\to\pi$.

We conclude from the discussions in Secs. III and IV that the leading-twist infrared structures in the processes $\pi\gamma^*\to\pi$ and $\pi\gamma^*\to\gamma$ are identical, and that the pion wave function, defined by Eq. (22), is universal.

V. FACTORIZATION OF B MESON DECAYS

In this section we present the all-order proof of factorization theorem for the exclusive B meson decays $B\to\gamma l\bar{\nu}$ and $B\to\pi l\bar{\nu}$ in the heavy quark limit. It will be shown that the proof for the pion transition form factor in Sec. III can be generalized to B meson decays, if terms suppressed by powers of $1/M_B$ are neglected. The momentum P_1 of the B meson and the momentum P_2 of the outgoing on-shell photon (pion) are parametrized as

$$P_1=\frac{M_B}{\sqrt{2}}(1,1,\mathbf{0}_T),\quad P_2=\frac{M_B}{\sqrt{2}}(0,\eta,\mathbf{0}_T), \tag{50}$$

where η denotes the energy fraction carried by the photon (pion). Assume that the light spectator quark in the B meson carries the momentum k, and that ϵ denotes the polarization vector of the photon. We consider the kinematic region with small q^2, $q=P_1-P_2$ being the lepton pair momentum, i.e., with large η, where PQCD is applicable. In the heavy quark limit the mass difference between the B meson and the b quark, $\bar{\Lambda}=M_B-m_b$, is a small scale, which will appear as higher-twist terms proportional to $\bar{\Lambda}/M_B$. The four components of the spectator quark momentum k are of the same order as $\bar{\Lambda}$.

The lowest-order diagrams for the $B\to\gamma l\bar{\nu}$ decay and for the $B\to\pi l\bar{\nu}$ decay are displayed in Fig. 1 and Fig. 5, respectively, but with the upper quark line replaced by a b quark line and with the vertex $\times$ representing a weak decay vertex. It is easy to observe that Figs. 1(a) and 1(b) scale like

$$H_{1a}^{(0)}\propto\frac{1}{(P_2-k)^2}\sim\frac{1}{\bar{\Lambda}M_B}, \tag{51}$$

$$H_{1b}^{(0)}\propto\frac{1}{(q-k)^2-M_B^2}\sim\frac{1}{M_B^2}, \tag{52}$$

indicating that Fig. 1(b) is power-suppressed. In the following analysis we shall concentrate only on Fig. 1(a). There are two leading-twist spin structures for the B meson,

$$\frac{(\not P_1+M_B)\bar{\not n}\gamma_5}{2\sqrt{N_c}},\quad\frac{(\not P_1+M_B)\not n\gamma_5}{2\sqrt{N_c}}, \tag{53}$$

with the dimensionless vecor $\bar{n}=(1,0,0_T)$, each of which is associated with a B meson wave function. For the radiative decay $B\to\gamma l\bar{\nu}$, only the first structure contributes at the leading-twist.

Contracting the amplitudes in Fig. 1(a) with $(\not P_1+M_B)\bar{\not n}\gamma_5/(2\sqrt{N_c})$, we derive

$$H_{1a}^{(0)}(x)=-e\frac{\sqrt{N_c}}{2}\frac{\mathrm{tr}[\not\epsilon\not P_2\gamma_\mu(1-\gamma_5)\not n]}{x\eta M_B}, \tag{54}$$

where $x=k^+/P_1^+$ is the momentum fraction. Since P_2 has been chosen in the minus direction, only the plus component k^+ of k is relevant. We have dropped the higher-twist terms proportional to k in the numerators and $\bar{\Lambda}$ by assuming $m_b\approx M_B$. It is then possible to integrate out the k^- and k_T dependences in the B meson wave function $\psi_+(k)$, leading to the light-cone B meson wave function,

$$\phi_+(x)=\int dk^-d^2k_T\psi_+(k). \tag{55}$$

It will be shown that a light-cone B meson wave function can always be defined, if an appropriate frame is chosen, even though the four components of k are of the same order.

A. $O(\alpha_s)$ factorization of $B\to\gamma l\bar{\nu}$

We start with the one-loop diagrams in Fig. 2 for the $B\to\gamma l\bar{\nu}$ decay, discussing the factorization of their infrared divergences. The factorization of Figs. 2(a)–2(c) requires the insertion of the Fierz identity. Take Fig. 2(b) as an example [the analysis of Figs. 2(a) and 2(c) is trivial]. The loop integrand is written as

$$\begin{aligned}I_{2b}\approx ig^2C_F\,\mathrm{tr}\Bigg\{&\gamma_\nu\frac{\not k-\not l}{(k-l)^2}\frac{\gamma_5\gamma^\alpha}{2}\\&\times\frac{\not P_1-\not k+\not l+M_B}{(P_1-k+l)^2-M_B^2}\gamma^\nu\frac{(\not v+I)\bar{\not n}\gamma_5}{2}\Bigg\}\frac{1}{l^2}\\&\times e\frac{\sqrt{N_c}}{2}\frac{\mathrm{tr}[\not\epsilon(\not P_2-\not k+\not l)\gamma_\mu(1-\gamma_5)M_B\gamma_\alpha\gamma_5]}{(P_2-k+l)^2},\end{aligned} \tag{56}$$

where we have kept only the leading-twist structure $\gamma_5\gamma^\alpha$ in the Fierz identity, and introduced the dimensionless vector $v=P_1/M_B$. The other structures, such as γ_5 and $\gamma_5\sigma^{\alpha\beta}$, do not contribute, because the corresponding hard amplitude vanishes:

$$e\frac{\sqrt{N_c}}{2}\frac{\mathrm{tr}[\not\epsilon(\not P_2-\not k+\not l)\gamma_\mu(1-\gamma_5)M_B\gamma_5]}{(P_2-k+l)^2}=0. \tag{57}$$

In the heavy quark limit we have the eikonal approximation,

$$\frac{\not P_1-\not k+\not l+M_B}{(P_1-k+l)^2-M_B^2}\gamma^\nu(\not v+I)\approx\frac{v^\nu}{v\cdot(l-k)}(\not v+I), \quad (58)$$

which is in fact equivalent to the heavy quark expansion. Obviously, only the component $\gamma_+=\gamma^-$ of γ_α contributes to the hard amplitude at leading twist, requiring the spin structure $\gamma_5\gamma^\alpha$ to be $\gamma_5\gamma^+$ in the first trace for the B meson wave function. Equation (56) becomes

$$I_{2b}\approx(\phi_+^{(1)})_{2b}H_{1a}^{(0)}(\xi), \quad (59)$$

with $\xi=x-l^+/P_1^+$ and the $O(\alpha_s)$ B meson wave function,

$$(\phi_+^{(1)})_{2b}=ig^2C_F tr\left\{\gamma_\nu\frac{\not k-\not l}{(k-l)^2}\frac{\gamma_5\gamma^+}{2}\frac{(\not v+I)\not{\bar n}\gamma_5}{2}\right\}\times\frac{1}{l^2}\frac{v^\nu}{v\cdot(l-k)}. \quad (60)$$

Figure 2(b) has been expressed as the convolution of the hard amplitude $H_{1a}^{(0)}$ with the $O(\alpha_s)$ infrared divergent diagrams, which contribute to $\phi_+^{(1)}$, in the momentum fraction ξ.

Equation (60) is simplified into

$$(\phi_+^{(1)})_{2b}=-ig^2C_F\frac{2v^-(l^+-k^+)}{(k-l)^2l^2v\cdot(l-k)}. \quad (61)$$

Performing the contour integration over, say, l^-, we observe that the integral is singular only when the component l^+ is of $O(\bar\Lambda)$. This observation implies that the infrared divergence associated with the B meson is of the soft type. This dynamics differs from the collinear type of divergences associated with the pion in the process $\pi\gamma^*\to\gamma$. It is easy to understand that the soft divergences in Figs. 2(a)–2(c) do not cancel in B meson decays [7]: The light spectator quark, carrying a small amount of momenta, forms a color cloud around the b quark. This cloud is also huge in space-time, such that soft gluons resolve the color structure of the B meson.

Diagrams with the additional gluon attaching the internal quark in Figs. 2(d) and 2(e) also contain soft divergences, since the internal quark is off-shell only by $O(\bar\Lambda M_B)$. Note that the internal quark in the process $\pi\gamma^*\to\gamma$ is off-shell by $O(Q^2)$. There is no collinear divergence from l parallel to P_2, because the internal quark propagator remains the scaling law $1/\bar\Lambda M_B$, instead of $1/\bar\Lambda^2$. The integrand associated with Fig. 2(d) is written as

$$I_{2d}=-ieg^2C_F\frac{\sqrt{N_c}}{2}\mathrm{tr}\left\{\not\epsilon\frac{\not P_2-\not k}{(P_2-k)^2}\gamma_\nu\frac{\not P_2-\not k+\not l}{(P_2-k+l)^2}\times\gamma_\mu(1-\gamma_5)\frac{\not P_1-\not k+\not l+M_B}{(P_1-k+l)^2-M_B^2}\gamma^\nu(\not P_1+M_B)\not{\bar n}\gamma_5\right\}\frac{1}{l^2}. \quad (62)$$

Inserting the Fierz identity, we have

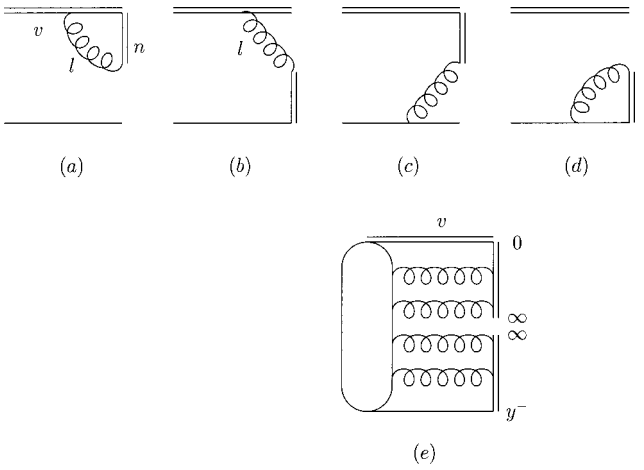

FIG. 8. (a)–(d) Infrared divergent diagrams factored out of Figs. 2(d) and 2(e) for the $B\to\gamma l\bar\nu$ decay. (e) The graphic definition of the leading-twist B meson wave function.

$$I_{2d}\approx-ig^2C_F\frac{2P_{2\nu}}{(P_2-k+l)^2}\mathrm{tr}\left\{\frac{\gamma_5\gamma^\alpha}{2}\frac{\not P_1-\not k+\not l+M_B}{(P_1-k+l)^2-M_B^2}\times\gamma^\nu\frac{(\not v+I)\not{\bar n}\gamma_5}{2}\right\}\frac{1}{l^2}e\frac{\sqrt{N_c}}{2}\frac{\mathrm{tr}[\not\epsilon\not P_2\gamma_\mu(1-\gamma_5)M_B\gamma_\alpha\gamma_5]}{(P_2-k)^2}. \quad (63)$$

Obviously, the first trace is proportional to $\bar n^\alpha$ in the heavy quark limit.

We employ the relation similar to Eq. (13),

$$\frac{2P_{2\nu}}{(P_2-k+l)^2}\approx\frac{n_\nu}{n\cdot l}\left[1-\frac{(P_2-k)^2}{(P_2-k+l)^2}\right], \quad (64)$$

where the terms $(k-l)^2\sim O(\bar\Lambda^2)$ and $k^2\sim O(\bar\Lambda^2)$ have been neglected. The eikonal line in the direction of n appears. Equation (63) reduces to

$$I_{2d}\approx(\phi_+^{(1)})_{2d}[H_{1a}^{(0)}(x)-H_{1a}^{(0)}(\xi)], \quad (65)$$

with the $O(\alpha_s)$ B meson wave function,

$$(\phi_+^{(1)})_{2d}=-ig^2C_F\frac{n_\nu}{n\cdot l}\mathrm{tr}\left\{\frac{\gamma_5\gamma^+}{2}\frac{(\not v+I)\not{\bar n}\gamma_5}{2}\right\}\frac{1}{l^2}\frac{v^\nu}{v\cdot(l-k)}. \quad (66)$$

The above expression implies that the infrared divergences in irreducible diagrams can also be collected by the eikonal line along the light cone. This is attributed to the choice of the frame, in which the photon moves in the minus direction. The first and second terms in Eq. (66) are described by Figs. 8(a) and 8(b), respectively, where the eikonal lines in the directions of v and of n have been indicated. In Fig. 8(b) the loop momentum l flows into the internal quark line, such that the second term appears as a convolution of $H_{1a}^{(0)}$ with $(\phi_+^{(1)})_{2d}$ in the momentum fraction ξ.

Figure 2(e) gives the loop integrand

$$I_{2e}=ieg^2C_F\frac{\sqrt{N_c}}{2}\mathrm{tr}\left\{\gamma^\nu\frac{\not k-\not l}{(k-l)^2}\not\epsilon\frac{\not P_2-\not k+\not l}{(P_2-k+l)^2}\gamma_\nu\right.$$
$$\left.\times\frac{\not P_2-\not k}{(P_2-k)^2}\gamma_\mu(1-\gamma_5)(\not P_1+M_B)\overline{\not n}\gamma_5\right\}\frac{1}{l^2}. \quad (67)$$

Inserting the Fierz identity, we have

$$I_{2e}\approx ig^2C_F\frac{2P_{2\nu}}{(P_2-k+l)^2}\mathrm{tr}\left\{\gamma^\nu\frac{\not k-\not l}{(k-l)^2}\frac{\gamma_5\gamma^\alpha}{2}\frac{(\not v+I)\overline{\not n}\gamma_5}{2}\right\}\frac{1}{l^2}$$
$$\times e\frac{\sqrt{N_c}}{2}\frac{\mathrm{tr}[\not\epsilon\not P_2\gamma_\mu(1-\gamma_5)M_B\gamma_\alpha\gamma_5]}{(P_2-k)^2}. \quad (68)$$

Similarly, the component $\gamma_+=\gamma^-$ of γ_α in the second trace is selected. Employing Eq. (64), the above expression is rewritten as

$$I_{2e}\approx-(\phi_+^{(1)})_{2e}[H_{1a}^{(0)}(\xi)-H_{1a}^{(0)}(x)], \quad (69)$$

with the $O(\alpha_s)$ B meson wave function

$$(\phi_+^{(1)})_{2e}=ig^2C_F\frac{n_\nu}{n\cdot l}\mathrm{tr}\left\{\gamma^\nu\frac{\not k-\not l}{(k-l)^2}\frac{\gamma_5\gamma^+}{2}\frac{(\not v+I)\overline{\not n}\gamma_5}{2}\right\}\frac{1}{l^2}. \quad (70)$$

We have split Fig. 2(e) into two terms, whose infrared divergent factors are described by Figs. 8(c) and 8(d), respectively.

Comparing Eqs. (60), (66), and (70), the Feynman rules for the perturbative evaluation of the B meson wave function are clear: $\phi_B^{(1)}$ can be written as a nonlocal hadronic matrix element with the structure $\gamma_5\gamma^+/2$ sandwiched:

$$\phi_+^{(1)}(x)=\frac{1}{\sqrt{2N_c}M_B}\int\frac{dy^-}{2\pi}e^{ixP_1^+y^-}\langle0|\overline{q}(y^-)\frac{\gamma_5\gamma^+}{2}(-ig)$$
$$\times\int_0^{y^-}dzn\cdot A(zn)b_v(0)|B(P_1)\rangle, \quad (71)$$

where the rescaled b quark field,

$$b_v(y)=\exp(iM_Bv\cdot y)\frac{\not v+I}{2}b(y), \quad (72)$$

has been introduced. The Feynman rules associated with b_v are those for an eikonal line in the direction of v given in Eq. (58). The above definition reproduces the contributions from Figs. 2(a)–2(c) and from Figs. 8(a)–8(d), if it is evaluated perturbatively.

The factorization formula for the $B\to\gamma l\overline{\nu}$ decay is written, up to $O(\alpha_s)$, as

$$(\phi_+^{(0)}+\phi_+^{(1)})\otimes(H_{1a}^{(0)}+H_{1a}^{(1)})+O(\alpha_s^2), \quad (73)$$

with $\phi_+^{(0)}=1$ and $\otimes$ representing the convolution in the momentum fraction. The $O(\alpha_s)$ hard amplitude $H_{1a}^{(1)}$ is defined by

$$H_{1a}^{(1)}\equiv\sum_i\int\frac{d^4l}{(2\pi)^4}I_i-\phi_+^{(1)}\otimes H_{1a}^{(0)}, \quad (74)$$

where the subscript i runs from $2a$ to $2e$. Obviously, $H_{1a}^{(1)}$ is infrared finite, since all the (α_s) soft divergences have been absorbed into the B meson wave function $\phi_+^{(1)}$.

B. All-order factorization of $B\to\gamma l\overline{\nu}$

We prove leading-twist factorization theorem for the $B\to\gamma l\overline{\nu}$ decay to all orders, and construct a gauge-invariant light-cone B meson wave function defined by

$$\phi_+(x)=\frac{1}{\sqrt{2N_c}M_B}\int\frac{dy^-}{2\pi}e^{ixP_1^+y^-}\langle0|\overline{q}(y^-)\frac{\gamma_5\gamma^+}{2}P$$
$$\times\exp\left[-ig\int_0^{y^-}dzn\cdot A(zn)\right]b_v(0)|B(P_1)\rangle, \quad (75)$$

as shown in Fig. 8(e). The eikonal lines in the directions of v and of n have been indicated. By expanding the light quark field $\overline{q}(y^-)$ and the path-ordered exponential into powers of y^-, the nonlocal matrix element can be expressed as a series of covariant derivatives $(D^+)^n\overline{q}(0)$, implying that Eq. (75) is gauge invariant.

We present the proof by induction. The factorization of the $O(\alpha_s)$ infrared divergences associated with the B meson has been worked out. Assume that the factorization of the infrared divergences holds up to $O(\alpha_s^N)$, that is, we have Eqs. (24)–(26) for the $B\to\gamma l\overline{\nu}$ decay. Consider a complete set of $O(\alpha_s^{N+1})$ full diagrams $G^{(N+1)}$. We look for the gluon, one of whose ends attaches the outer most vertex on the b quark line. We classify $G^{(N+1)}$ into the reducible and irreducible types as in Sec. III. The factorization of the reducible $G^{(N+1)}$ is the same as that of Figs. 2(a)–2(c): Following Eqs. (56)–(60), we insert the Fierz identity to separate the reducible $G^{(N+1)}$ into the convolution of $G^{(N)}$ with the $O(\alpha_s)$ infrared divergent diagrams, which contribute to the B meson wave function $\phi_B^{(1)}$. The result is similar to that shown in Fig. 4(a).

For the factorization of the irreducible diagrams, we rely on the Ward identity in Eq. (23). In this case the amplitude G^μ contains two on-shell external quarks, one of which is the heavy b quark. As hinted by the $O(\alpha_s)$ analysis, the soft divergence, associated with the gluon radiated by the outer most vertex on the b quark line, can be collected by the eikonal approximation, i.e., by the replacement in Eq. (27). The reason is as follows. In the heavy quark limit the full diagrams of the $B\to\gamma l\overline{\nu}$ decay are dominated by the momentum flow along the photon momentum P_2 in the minus direction. Strickly speaking, they are dominated by P_2-k. Hence, the vertex β inside $G^{(N)}$ the radiated gluon attaches is mainly minus, and the vertex α on the b quark line is

mainly plus. Apparently, the tensor $n_\alpha l_\beta / n\cdot l$ extracts the correct leading contribution. Therefore, we have the equation described by Fig. 4(b).

The second and third diagrams in Fig. 4(b) give

$$l_\beta \frac{1}{\not P_1 - \not k - \not l - M_B}\gamma^\beta (\not l + I)\bar{\not n}\gamma_5 = -\frac{1}{\not P_1 - \not k - \not l - M_B}\not k(\not l + I)\bar{\not n}\gamma_5 - (\not l + I)\bar{\not n}\gamma_5, \tag{76}$$

$$l_\beta (\not l + I)\bar{\not n}\gamma_5\gamma^\beta \frac{1}{\not k - \not l} = (\not l + I)\bar{\not n}\gamma_5 \not k \frac{1}{\not k - \not l} - (\not l + I)\bar{\not n}\gamma_5, \tag{77}$$

respectively. After assigning the quark propagators on the right-hand sides of the above expressions into the corresponding loop integrals, the first terms are proportional to $k \sim O(\bar{\Lambda})$. They are suppressed by $O(\bar{\Lambda}/M_B)$ compared to the second terms, which correspond to $G^{(N)}$. Neglecting the higher-twist terms, the irreducible $G^{(N+1)}$ are factorized into the convolution of $G^{(N)}$ with the $O(\alpha_s)$ B meson wave function, in which the radiated gluon attaches the eikonal lines as in Figs. 8(a) and 8(b). The factorization of the irreducible $G^{(N+1)}$, with the gluon emitted from the outer most vertex on the light spectator quark line, is similar. The resultant $O(\alpha_s)$ infrared divergent diagrams for the B meson wave function are those in Figs. 8(c) and 8(d).

Combining the factorizations of the reducible and irreducible $G^{(N+1)}$, we arrive at Eq. (31). The factorization in Eq. (32) for the B meson wave function $\phi_+^{(N+1)}$ also exists. Following the steps in Eqs. (33)–(35), we complete the all-order proof of leading-twist factorization theorem for the $B \to \gamma l \bar{\nu}$ decay. The definition of the hard amplitude at each order is the same as in Eq. (34). Since the full diagrams are dominated by momenta along P_2, only the plus component k^+ of k is relevant in the hard amplitude. This is the reason we can integrate the B meson wave function over k^- and k_T, obtaining the light-cone B meson wave function in Eq. (75).

C. Factorization of $B \to \pi l \bar{\nu}$

The factorization of the pion wave function in Secs. II, III, IV, and the factorization of the B meson wave function in the $B \to \gamma l \bar{\nu}$ decay can be applied to the $B \to \pi l \bar{\nu}$ decay straightforwardly. Here we simply explain some points of the proof, and neglect the details. The lowest-order diagrams are shown in Fig. 5. Both the spin structures in Eq. (53) contribute to Fig. 5(b), but only the first one contributes to Fig. 5(a). Since P_2 has been chosen in the minus direction, only the plus component k^+ of k is relevant. It is then possible to define a light-cone B meson wave function for the $B \to \pi l \nu$ decay. We first identify infrared divergences from $O(\alpha_s)$ radiative corrections to Fig. 5(a), which are displayed in Fig. 6, since their analysis is similar to that of the $B \to \gamma l \bar{\nu}$ decay. Note that Fig. 6 is complete only for the construction of the B meson wave function. We do not consider self-energy corrections to the internal lines, which give only next-to-leading-order hard amplitudes.

The construction of the pion wave function is basically the same as that for the process $\pi\gamma^* \to \pi$. That is, the infrared divergences associated with the outgoing pion is of the collinear type. Soft divergences cancel by pairs, because soft gluons do not interact with the color singlet pion. For example, soft divergences cancel between Figs. 6(h) and 6(i) and between Figs. 6(j) and 6(k). The collinear gluons are still collected by the eikonal lines along the light cone, even though they may attach the heavy b quark. The reason is that when a loop momentum l is parallel to the pion momentum P_2 in the minus direction, only the component γ^+ of the vertex on the b quark line and P_1^+ of the B meson momentum are selected. Consequently, we derive the definition for the pion wave function, which is identical to Eq. (22). This conclusion is consistent with the universality of hadron wave functions.

We then concentrate on the B meson wave function. The treatment of the reducible diagrams in Figs. 6(a)–6(c) is exactly the same as in Figs. 2(a)–2(c) for the $B \to \gamma l \bar{\nu}$ decay. We insert the Fierz identity to separate these diagrams into the convolution of Fig. 5(a) with the $O(\alpha_s)$ soft divergent diagrams, which contribute to the B meson wave function $\phi_+^{(1)}$. The investigation of the irreducible diagrams in Figs. 6(d) and 6(e) hints that the soft divergences can be collected by the eikonal lines along the direction of n, a conclusion similar to that for Figs. 2(d) and 2(e). Hence, the replacement in Eq. (27) for the loop gluon extracts the soft divergences of the irreducible diagrams in Figs. 6(d)–6(k). The Ward identity applies, and the sum of these irreducible diagrams is factorized into the convolution of Fig. 5(a) with part of $\phi_+^{(1)}$ described by Figs. 8(a)–8(d). Following the procedures in Sec. III, we prove leading-twist factorization theorem for Fig. 5(a) in the $B \to \pi l \bar{\nu}$ decay. The B meson wave functions ϕ_+ constructed from the $B \to \gamma l \bar{\nu}$ and $B \to \pi l \bar{\nu}$ decays are identical.

The discussion of the $O(\alpha_s)$ radiative corrections to Fig. 5(b) shown in Fig. 7 is similar, though more complicated. The soft approximation, the Fierz insertion, and the Ward identity apply. Because of the existence of the heavy quark propagator, the spin structures $\gamma_5\gamma^\alpha$, γ_5, and $\gamma_5\sigma^{\alpha\beta}$ in the Fierz identity contribute. In this case two leading-twist B meson wave functions can be constructed [8]. Besides ϕ_+ defined in Eq. (75), we derive the additional light-cone B meson wave function associated with the structure $(\not P_1 + M_B)\bar{\not n}\gamma_5/(2\sqrt{N_c})$,

$$\phi_-(x) = \frac{1}{\sqrt{2N_c}M_B}\int \frac{dy^-}{2\pi} e^{ixP_1^+ y^-}\langle 0|\bar{q}(y^-)\frac{\gamma_5\gamma^-}{2}P \times \exp\left[-ig\int_0^{y^-} dz n\cdot A(zn)\right] b_v(0)|B(P_1)\rangle. \tag{78}$$

In summary, the nonlocal hadronic matrix element for the B meson is expressed as

$$\int \frac{dy^-}{2\pi} e^{ixP_1^+ y^-} \langle 0|\bar{q}_\gamma(y^-) b_\beta(0)|B(P_1)\rangle = -\left\{ \frac{(\not P_1 + M_B)}{\sqrt{2N_c}} \left[\frac{\bar{\not n}}{\sqrt{2}} \phi_+(x) + \frac{\not n}{\sqrt{2}} \phi_-(x) \right] \gamma_5 \right\}_{\gamma\beta}. \tag{79}$$

This result is exactly the same as that obtained in [8] at leading twist.

A remark is in order. The hard amplitude from Fig. 5(b), proportional to $1/(x_1 x_2^2)$, x_2 being the momentum fraction associated with the pion, develops an infrared singularity, if the pion wave function vanishes like x_2 as $x_2\to 0$ [14]. Even though we have proved leading-twist factorization theorem for the $B\to\pi l\bar{\nu}$ decay, its practical application is questionable. It has been shown that the inclusion of parton transverse momenta k_T smears the singularities from the end-point region of momentum fractions [7]. When k_T is included, the dependence on the transverse loop momentum l_T, being of the same order as k_T, is not negligible in the hard amplitude. This complexity can be resolved by Fourier transforming the factorization formula from the k_T space into the b space, where b is the impact parameter conjugate to k_T [15,16]. The l_T dependence then appears in the factor $\exp(-i\mathbf{l}_T\cdot\mathbf{b})$, and decouples from the hard amplitude. This factor can be assigned into the corresponding loop integral, which contributes to the definition of the meson wave functions. We claim that the factorization of the $B\to\pi l\bar{\nu}$ decay must be performed in the impact parameter space [17].

VI. CONCLUSION

In this paper we have investigated the infrared divergences in the processes $\pi\gamma^*\to\gamma$ and $\pi\gamma^*\to\pi$. We summarize their comparision below. There are no soft divergences, since they are either absent or cancel among sets of diagrams. In the collinear region with l parallel to P_1, Figs. 2(a)–2(c) are identical to Figs. 6(a)–6(c) [Figs. 7(a)–7(c)]. Figures 2(d) and 2(e) are identical to the combination of Figs. 6(d)–6(k) [Figs. 7(d)–7(k)]. That is, the collinear structures are the same at the leading twist, consistent with the concept of universality of hadron wave functions in PQCD factorization theorem. However, due to the potential significant subleading contributions at low energies, the extraction of the leading-twist pion wave function from the $\pi\gamma^*\to\gamma(\pi)$ data suffers ambiguity. For details, refer to Appendix B.

We have presented an all-order proof of leading-twist factorization theorem for the processes $\pi\gamma^*\to\gamma$ and $\pi\gamma^*\to\pi$, and for the decays $B\to\gamma l\bar{\nu}$ and $B\to\pi l\bar{\nu}$ by means of the Ward identity. The small scales, such as the light spectator quark momentum k and the B meson and b quark mass difference $\bar{\Lambda}$, are neglected in the heavy quark limit, such that the Ward identity holds. Our proof is simple compared to that in [4], and explicitly gauge invariant, compared to that in [1]. We have constructed the gauge-invariant pion and B meson wave functions, and confirmed their universality. The path-ordered integral appears as a consequence of the Ward idenity. Note the difference between the definitions for the pion and B meson wave functions. The former, collecting the collinear divergences, depends on the structure $\gamma_5\gamma^+$. The latter, collecting the soft divergences, depends on the structure $\gamma_5\not b$. We emphasize that it is possible to define a light-cone B meson wave function, if an appropriate frame is chosen, in which the photon (pion) moves in the minus or plus direction. This is also the reason we can extract the infrared divergences in $\pi\gamma^*\to\gamma(\pi)$ and $B\to\gamma(\pi)l\bar{\nu}$ using the same replacement in Eq. (27).

The leading-twist factorization of the $B\to\pi l\bar{\nu}$ decay can be proved straightforwardly, following the procedures presented in Secs. II–V. However, for a practical application, the parton transverse momenta k_T must be included in order to smear the end-point singularities in the hard amplitude. We shall derive factorization theorem including these additional degrees of freedom elsewhere [17]. Our proof will be generalized to nonleptonic B meson decays, such as $B\to\pi\pi$. This factorization is more complicated, since nonleptonic decays involve three characteristic scales: the W boson mass M_W, M_B, and small scales of $O(\bar{\Lambda})$, such as k_T.

ACKNOWLEDGMENTS

I thank S. Brodsky, S. Dorokhov, T. Morozumi, M. Nagashima, D. Pirjol, A.I. Sanda, and G. Sterman for useful discussions. This work was supported in part by the National Science Council of R.O.C. under the Grant No. NSC-89-2112-M-006-033, by Grant-in Aid for Special Project Research (Physics of CP Violation) from the Ministry of Education, Science and Culture and by Hiroshima University, Japan.

APPENDIX A: $O(\alpha_s)$ COLLINEAR CORRECTIONS

In this appendix we supply the details of the derivation of the collinear divergences in the process $\pi\gamma^*\to\pi$. The loop integrand from Fig. 6(d) is written as

$$I_{6d} = \frac{-ieg^4}{2N_c}\mathrm{tr}\left\{ \gamma^\lambda\gamma_5 \not P_2 \gamma^\beta \frac{\not P_2 - x_1\not P_1 + \not l}{(P_2 - x_1P_1 + l)^2} \times \gamma_\mu \frac{(1-x_1)\not P_1 + \not l}{[(1-x_1)P_1 + l]^2} \times \gamma^\alpha \not P_1 \gamma_5 \right\} \times \frac{\mathrm{tr}(T^a T^b T^c)\Gamma^{abc}_{\alpha\beta\lambda}}{l^2(x_1P_1 - x_2P_2 - l)^2(x_1P_1 - x_2P_2)^2}, \tag{A1}$$

with N_c being the number of colors and the triple-gluon vertex,

$$\Gamma^{abc}_{\alpha\beta\lambda} = -f^{abc}[g_{\alpha\beta}(2l - x_1P_1 + x_2P_2)_\lambda + g_{\beta\lambda}(2x_1P_1 - 2x_2P_2 - l)_\alpha + g_{\lambda\alpha}(x_2P_2 - x_1P_1 - l)_\beta], \tag{A2}$$

f^{abc} being a antisymmetric tensor. In the collinear region with l parallel to P_1, only the term proportional to $g_{\beta\lambda}$ is important, since the terms proportional to $g_{\lambda\alpha}$ and $g_{\alpha\beta}$, giving

$$\begin{aligned}&[(1-x_1)\not P_1+\not l]\gamma^\alpha \not P_1\gamma_5\gamma^\lambda g_{\lambda\alpha}\\&\quad=2P_1\cdot[(1-x_1)P_1+l]\gamma_5\\&\quad\sim O(\lambda^2),\gamma^\alpha\not P_1\gamma_5(2\not l-x_1\not P_1+x_2\not P_2)\gamma_5\not P_2\gamma^\beta g_{\alpha\beta}\\&\quad=2P_1\cdot(2l-x_1P_1)\not P_2\sim O(\lambda^2)\not P_2,\end{aligned}\tag{A3}$$

do not produce collinear divergences. Considering the second term in Eq. (A2), Eq. (A1) exhibits the collinear divergence

$$I_{6d}\approx\frac{-3ig^2P_2\cdot[(1-x)P_1+l]}{[(1-x)P_1+l]^2l^2[P_2\cdot(l-xP_1)]}H_{5a}^{(0)},\tag{A4}$$

where we have employed the identities

$$tr(T^aT^bT^c)=\frac{1}{4}(d^{abc}+if^{abc}),\quad d^{abc}f^{abc}=0,$$

$$f^{abc}f^{abc}=24,\tag{A5}$$

d^{abc} being a symmetric tensor, and the approximation for the denominator

$$(x_1P_1-x_2P_2-l)^2=2x_2P_2\cdot(l-x_1P_1).\tag{A6}$$

It is found that the infrared divergent piece of the radiative correction has been completely factored out. The remaining part, denoted by the lowest-order hard amplitude $H_{5a}^{(0)}$, does not depend on the loop momentum l at all.

Figure 6(e) gives the loop integrand

$$\begin{aligned}I_{6e}=\frac{ieg^4}{2N_c}\mathrm{tr}\Bigg\{&\gamma^\alpha\frac{x_1\not P_1-\not l}{(x_1P_1-l)^2}\gamma^\lambda\gamma_5\not P_2\gamma^\beta\frac{\not P_2-x_1\not P_1}{(P_2-x_1P_1)^2}\\&\times\gamma_\mu\not P_1\gamma_5\Bigg\}\frac{\mathrm{tr}(T^aT^bT^c)\Gamma^{abc}_{\alpha\beta\lambda}}{l^2(x_1P_1-x_2P_2-l)^2(x_1P_1-x_2P_2)^2},\end{aligned}\tag{A7}$$

with the triple-gluon vertex,

$$\begin{aligned}\Gamma^{abc}_{\alpha\beta\lambda}=-f^{abc}[&g_{\alpha\beta}(l-x_1P_1+x_2P_2)_\lambda+g_{\beta\lambda}(2x_1P_1-2x_2P_2\\&+l)_\alpha+g_{\lambda\alpha}(x_2P_2-x_1P_1-2l)_\beta].\end{aligned}\tag{A8}$$

Similarly, in the region with l parallel to P_1 we have

$$I_{6e}\approx\frac{-3ig^2}{(x_1P_1-l)^2l^2}H_{5a}^{(0)}.\tag{A9}$$

The integrand associated with Fig. 6(f) is written as

$$\begin{aligned}I_{6f}=\frac{eg^4C_F^2}{2}\mathrm{tr}\Bigg\{&\gamma_\alpha\gamma_5\not P_2\gamma^\alpha\frac{\not P_2-x_1\not P_1}{(P_2-x_1P_1)^2}\\&\times\gamma_\nu\frac{\not P_2-x_1\not P_1+\not l}{(P_2-x_1P_1+l)^2}\gamma_\mu\frac{(1-x_1)\not P_1+\not l}{[(1-x_1)P_1+l]^2}\gamma^\nu\not P_1\gamma_5\Bigg\}\\&\times\frac{1}{l^2(x_1P_1-x_2P_2)^2},\end{aligned}\tag{A10}$$

which is simplified into

$$\begin{aligned}I_{6f}=&-2eg^4C_F^2\\&\times\frac{\mathrm{tr}[\gamma_\mu(\not P_2+\not l)\not P_1\not l]}{[(1-x_1)P_1+l]^2(P_2-x_1P_1+l)^2l^2(x_1P_1-x_2P_2)^2}.\end{aligned}\tag{A11}$$

The trace in the above expression is proportional to the vanishing factor $P_1\cdot l$, which suppresses the divergence from the denominator $[(1-x_1)P_1+l]^2$. Figure 6(g) does not contain collinear divergences for the same reason.

The loop integrand associated with Fig. 6(h) is written as

$$\begin{aligned}I_{6h}=-\frac{eg^4C_F}{4N_c}\mathrm{tr}\Bigg\{&\gamma_\alpha\gamma_5\not P_2\gamma_\nu\frac{(1-x_2)\not P_2+\not l}{[(1-x_2)P_2+l]^2}\\&\times\gamma^\alpha\frac{\not P_2-x_1\not P_1+\not l}{(P_2-x_1P_1+l)^2}\gamma_\mu\frac{(1-x_1)\not P_1+\not l}{[(1-x_1)P_1+l]^2}\gamma^\nu\not P_1\gamma_5\Bigg\}\\&\times\frac{1}{l^2(x_1P_1-x_2P_2)^2},\end{aligned}\tag{A12}$$

which is simplified into

$$\begin{aligned}I_{6h}=-\frac{2eg^4C_F}{N_c}&\frac{P_1\cdot[(1-x_2)P_2+l]}{[(1-x_2)P_2+l]^2}\\&\times\mathrm{tr}\Bigg\{\not P_2\frac{\not P_2-x_1\not P_1+\not l}{(P_2-x_1P_1+l)^2}\gamma_\mu\frac{(1-x_1)\not P_1+\not l}{[(1-x_1)P_1+l]^2}\Bigg\}\\&\times\frac{1}{l^2(x_1P_1-x_2P_2)^2}.\end{aligned}\tag{A13}$$

In the region with l parallel to P_1, we have the approximation

$$\begin{aligned}I_{6h}&\approx\frac{ig^2}{N_c}\frac{P_2\cdot[(1-x_1)P_1+l]}{[(1-x_1)P_1+l]^2l^2P_2\cdot l}H_{4a}^{(0)}\\&=\frac{ig^2}{N_c}\frac{n\cdot[(1-x_1)P_1+l]}{[(1-x_1)P_1+l]^2l^2n\cdot l}H_{5a}^{(0)},\end{aligned}\tag{A14}$$

where we have adopted the approximation for the quark propagator $[(1-x_2)P_2+l]\approx2(1-x_2)P_2\cdot l$, and dropped all the terms proportional to $P_1\cdot l$.

The loop integrand corresponding to Fig. 6(i) is written as

$$I_{6i}=\frac{eg^4C_F}{4N_c}\mathrm{tr}\Big\{\gamma_\alpha\frac{x_2\not P_2+\not l}{(x_2P_2+l)^2}\gamma_\nu\gamma_5\not P_2\gamma^\alpha\frac{\not P_2-x_1\not P_1+\not l}{(P_2-x_1P_1+l)^2}\gamma_\mu \times\frac{(1-x_1)\not P_1+\not l}{[(1-x_1)P_1+l]^2}\gamma^\nu\not P_1\gamma_5\Big\}\frac{1}{l^2(x_1P_1-x_2P_2-l)^2}, \tag{A15}$$

whose sign is opposite to that of Eq. (A12) due to the antiquark propagator. The above expression is simplified into

$$I_{6i}=\frac{2eg^4C_F}{N_c}\mathrm{tr}\Big\{\frac{x_2\not P_2+\not l}{(x_2P_2+l)^2}\frac{\not P_2-x_1\not P_1+\not l}{(P_2-x_1P_1+l)^2}\gamma_\mu \times\frac{(1-x_1)\not P_1+\not l}{[(1-x_1)P_1+l]^2}\Big\}\frac{P_1\cdot P_2}{l^2(x_1P_1-x_2P_2-l)^2}. \tag{A16}$$

It is easy to derive the collinear approximation,

$$I_{6i}\approx\frac{-ig^2}{N_c}\frac{n\cdot[(1-x_1)P_1+l]}{[(1-x_1)P_1+l]^2l^2n\cdot l}\frac{(x_1P_1-x_2P_2)^2}{(x_1P_1-x_2P_2-l)^2}H_{5a}^{(0)}. \tag{A17}$$

The similar procedures apply to Figs. 6(j) and 6(k).

The integrand associated with Fig. 7(f) is written as

$$I_{7f}=-\frac{eg^4C_F}{4N_c}\mathrm{tr}\Big\{\gamma_\alpha\gamma_5\not P_2\gamma_\mu\frac{\not P_1-x_2\not P_2}{(P_1-x_2P_2)^2} \times\gamma_\nu\frac{\not P_1-x_2\not P_2+\not l}{(P_1-x_2P_2+l)^2}\gamma^\alpha\frac{(1-x_1)\not P_1+\not l}{[(1-x_1)P_1+l]^2}\gamma^\nu\not P_1\gamma_5\Big\} \times\frac{1}{l^2(x_1P_1-x_2P_2)^2}, \tag{A18}$$

which is simplified into

$$I_{7f}=-\frac{2eg^4C_F}{N_c}\frac{P_1\cdot(l-x_2P_2)}{(P_1-x_2P_2+l)^2}\mathrm{tr}\Big\{\not P_2\gamma_\mu\frac{\not P_1-x_2\not P_2}{(P_1-x_2P_2)^2} \times\frac{(1-x_1)\not P_1+\not l}{[(1-x_1)P_1+l]^2}\Big\}\frac{1}{l^2(x_1P_1-x_2P_2)^2}. \tag{A19}$$

In the collinear region we have the approximation

$$I_{7f}\approx\frac{ig^2}{N_c}\frac{P_2\cdot[(1-x_1)P_1+l]}{[(1-x_1)P_1+l]^2l^2P_2\cdot(P_1+l)}H_{5b}^{(0)}. \tag{A20}$$

The integrand corresponding to Fig. 7(h) is written as

$$I_{7h}=-\frac{eg^4C_F}{4N_c}\mathrm{tr}\Big\{\gamma_\alpha\gamma_5\not P_2\gamma_\nu\frac{(1-x_2)\not P_2+\not l}{[(1-x_2)P_2+l]^2} \times\gamma_\mu\frac{\not P_1-x_2\not P_2+\not l}{(P_1-x_2P_2+l)^2}\gamma^\alpha\frac{(1-x_1)\not P_1+\not l}{[(1-x_1)P_1+l]^2}\gamma^\nu\not P_1\gamma_5\Big\} \times\frac{1}{l^2(x_1P_1-x_2P_2)^2}, \tag{A21}$$

which is simplified into

$$I_{7h}=-\frac{2eg^4C_F}{N_c}\frac{P_2\cdot[(1-x_1)P_1+l]}{[(1-x_1)P_1+l]^2}\mathrm{tr}\Big\{\frac{(1-x_2)\not P_2+\not l}{[(1-x_2)P_2+l]^2}\gamma_\mu \times\frac{\not P_1-x_2\not P_2+\not l}{(P_1-x_2P_2+l)^2}\not P_1\Big\}\frac{1}{l^2(x_1P_1-x_2P_2)^2}. \tag{A22}$$

We have the collinear approximation,

$$I_{7h}\approx\frac{ig^2}{N_c}\frac{P_2\cdot[(1-x_1)P_1+l]}{[(1-x_1)P_1+l]^2l^2P_2\cdot(P_1+l)}\frac{P_1\cdot P_2}{P_2\cdot l}H_{5b}^{(0)}. \tag{A23}$$

APPENDIX B: DETERMINATION OF THE PION WAVE FUNCTION

In this appendix we comment on the determination of the leading-twist pion wave function, which can be parametrized as

$$\phi(x)=\frac{3f_\pi}{\sqrt{2N_c}}x(1-x)\Big[1+\frac{3}{2}c(5(1-2x)^2-1)\Big], \tag{B1}$$

with the shape parameter c. It has been proposed to extract the leading-twist pion wave function from experimental data of the pion transition form factor [18]. The asymptotic model was obtained with the shape parameter $c\sim0$,

$$\phi^{AS}(x)=\frac{3f_\pi}{\sqrt{2N_c}}x(1-x). \tag{B2}$$

The pion wave function can also be determined from other processes involving pions, such as the pion form factor and the B meson decays $B\to\pi l\bar{\nu}$ and $B\to D\pi$. It has been known that a large value of c is preferred for explaining the data of the pion form factor [15].

Another quantity that has been considered is the ratio of the branching ratios of the $B\to D\pi$ decays [19,20],

$$R\equiv\frac{B(B^+\to D^0\pi^+)}{B(B^0\to D^-\pi^+)}. \tag{B3}$$

The charged B meson decay contains both factorizable and nonfactorizable amplitudes: the $B\to D$ form factor associated with the external-W emission, the $B\to\pi$ form factor associated with the internal-W emission, and the nonfactorizable

amplitude associated with the internal-W emission. The neutral B meson decay contains only the factorizable external-W emission amplitude. The Wilson coefficient for the factorizable internal-W emission amplitude is small at scales around the b quark mass. Hence, the difference between the branching ratios $B(B^+\to D^0\pi^+)$ and $B(B^0\to D^-\pi^+)$ is attributed to the nonfactorizable internal-W emission amplitude. To explain the data of $R\sim 1.6$, a larger $c\sim 0.5$ has been obtained [21]. This value of c is located between those for the asymptotic model and for the Chernyak-Zhinitsky (CZ) model corresponding to $c=2/3$ [22],

$$\phi^{\rm CZ}(x)=\frac{5\sqrt{6}f_\pi}{2}x(1-x)(1-2x)^2. \tag{B4}$$

Note that the coefficient $c=0.44$ (at the factorization scale about 1 GeV) derived from QCD sum rules [23] is close to that extracted from the ratio R. However, also note that a flat pion wave function was concluded in the framework of covariant quark-pion model [24] and of QCD sum rules [25,26].

The above results seem not to be well consistent with the universality of the pion wave function. We emphasize that the infrared structures of the processes $\pi\gamma^*\to\gamma$ and $\pi\gamma^*\to\pi$ are different at next-to-leading twist. For example, the collinear divergences associated with the pseudoscalar structure γ_5 are absent in $\pi\gamma^*\to\gamma$, but exist in $\pi\gamma^*\to\pi$. The three-parton wave functions contribute to both the pion transition form factor and the pion form factor. It is expected that at the maximal energy scales around 8 GeV^2, where data are available, these subleading contributions are sizeable relative to the leading ones. It has been explicitly demonstrated that if higher-twist contributions from parton transverse momenta are taken into account, the CZ wave function is not excluded by the data of the pion transition form factor [27], contrary to the conclusion in [18]. It has been shown that the pion form factor suffers substantial higher-twist contributions proportional to the chiral condensate at currently available energy scales [28]. The $B\to\pi$ transition form factor also receives nonvanishing higher-twist contributions [29]. Because of these next-to-leading-twist ambiguity, we argue that the above different extractions of the leading-twist pion wave function should not be regarded as an inconsistency.

[1] S. J. Brodsky and G. P. Lepage, Phys. Lett. **87B**, 359 (1979); Phys. Rev. Lett. **43**, 545 (1979); G. P. Lepage and S. Brodsky, Phys. Rev. D **22**, 2157 (1980).

[2] S. J. Brodsky, Y. Frishman, G. P. Lepage, and C. Sachrajda, Phys. Lett. **91B**, 239 (1980).

[3] A. V. Efremov and A. V. Radyushkin, Theor. Math. Phys. **42**, 97 (1980); Phys. Lett. **94B**, 245 (1980); I. V. Musatov and A. V. Radyushkin, Phys. Rev. D **56**, 2713 (1997).

[4] A. Duncan and A. H. Mueller, Phys. Lett. **90B**, 159 (1980); Phys. Rev. D **21**, 1636 (1980).

[5] W. Zimmermann, *Elementary Particles in Quantum Field Theory* (MIT Press, Cambridge, MA, 1971).

[6] G. P. Korchemsky, D. Pirjol, and T. M. Yan, Phys. Rev. D **61**, 114510 (2000).

[7] H-n. Li and H. L. Yu, Phys. Rev. Lett. **74**, 4388 (1995); Phys. Lett. B **353**, 301 (1995); Phys. Rev. D **53**, 2480 (1996).

[8] A. G. Grozin and M. Neubert, Phys. Rev. D **55**, 272 (1997); M. Beneke and T. Feldmann, Nucl. Phys. **B592**, 3 (2000).

[9] F. Del Aguila and M. K. Chase, Nucl. Phys. **B193**, 517 (1981).

[10] E. Braaten, Phys. Rev. D **28**, 524 (1983).

[11] E. P. Kadantseva, S. V. Mikhailov, and A. V. Radyushkin, Yad. Fiz. **44**, 507 (1986) [Sov. J. Nucl. Phys. **44**, 326 (1986)].

[12] C. Becchi, A. Rouet, and R. Stora, Phys. Lett. **52B**, 344 (1974).

[13] B. Melic, B. Nizic, and K. Passek, Phys. Rev. D **60**, 074004 (1999), and references therein.

[14] R. Ahkoury, G. Sterman, and Y. P. Yao, Phys. Rev. D **50**, 358 (1994).

[15] H-n. Li and G. Sterman, Nucl. Phys. **B381**, 129 (1992).

[16] J. Botts and G. Sterman, Nucl. Phys. **B225**, 62 (1989).

[17] H-n. Li (in preparation).

[18] P. Kroll and M. Raulfs, Phys. Lett. B **387**, 848 (1996); S. J. Brodsky, C.-R. Ji, A. Pang, and D. G. Robertson, Phys. Rev. D **57**, 245 (1998).

[19] T. W. Yeh and H.-n. Li, Phys. Rev. D **56**, 1615 (1997).

[20] H-n. Li and B. Melic, Eur. Phys. J. C **11**, 695 (1999).

[21] C. D. Lu and H-n. Li (in preparation).

[22] V. L. Chernyak and A. R. Zhitnitsky, Phys. Rep. **112**, 173 (1984).

[23] V. M. Braun and I. E. Filyanov, Z. Phys. C **48**, 239 (1990); P. Ball, J. High Energy Phys. **01**, 010 (1999).

[24] I. V. Anikin, A. E. Dorokhov, and L. Tomio, Phys. Lett. B **475**, 361 (2000).

[25] A. P. Bakulev and S. V. Mikhailov, Z. Phys. C **68**, 451 (1995); Mod. Phys. Lett. A **11**, 1611 (1996).

[26] S. V. Mikhailov and A. V. Radyushkin, Phys. Rev. D **45**, 1754 (1992).

[27] F. G. Cao, T. Huang, and B. Q. Ma, Phys. Rev. D **53**, 6582 (1996).

[28] F. G. Cao, Y. B. Dai, and C. S. Huang, Eur. Phys. J. C **11**, 501 (1999).

[29] Y. Y. Keum, H-n. Li, and A. I. Sanda, Phys. Lett. B **504**, 6 (2001); Phys. Rev. D **63**, 054008 (2001); Y. Y. Keum and H-n. Li, *ibid.* **63**, 074006 (2001).